Biogeosciences Discuss., 12, 1247–1283, 2015
www.biogeosciences-discuss.net/12/1247/2015/
doi:10.5194/bgd-12-1247-2015

Biogeosciences Discussions
Open Access

Downward particle flux and carbon export in the Beaufort Sea, Arctic Ocean; the Malina experiment

J.-C. Miquel[1], B. Gasser[1], J. Martín[1,2], C. Marec[3], M. Babin[3], L. Fortier[3], and A. Forest[3]

[1]International Atomic Energy Agency, Environment Laboratories, 4, quai Antoine 1er, 98000 Monaco
[2]Institut de Ciències del Mar, Departament de Geologia Marina, Passeig Marítim de la Barceloneta, 37–49, 080030 Barcelona, Spain
[3]*Takuvik* Joint International Laboratory, Université de Laval (Canada) – CNRS (France), Département de Biologie and Québec-Océan, Université Laval, G1V 0A6, Canada

Received: 30 November 2014 – Accepted: 1 December 2014 – Published: 16 January 2015

Correspondence to: J.-C. Miquel (j.c.miquel@iaea.org)

Published by Copernicus Publications on behalf of the European Geosciences Union.

Abstract

As part of the international, multidisciplinary project Malina, downward particle fluxes were investigated by means of a drifting multi-sediment trap mooring deployed at three sites in the Canadian Beaufort Sea in late summer 2009. Mooring deployments lasted for 28–50 h and targeted the shelf-break and the slope along the Beaufort–Mackenzie continental margin, as well as the edge between the Mackenzie Shelf and the Amundsen Gulf. Besides analyses of C and N, the collected material was investigated for pigments, phyto- and microzooplankton, faecal pellets and swimmers.

The measured fluxes were relatively low, in the range of 11–54 mg m^{-2} d^{-1} for the total mass, 1–15 mg C m^{-2} d^{-1} for organic carbon and 0.2–2.5 mg N m^{-2} d^{-1} for nitrogen. Comparison with a long-term trap dataset from the same sampling area showed that the short-term measurements were at the lower end of the high variability characterizing a rather high flux regime during the study period.

The sinking material consisted of aggregates and particles that were characterized by the presence of hetero- and autotrophic microzooplankters and diatoms and by the corresponding pigment signatures. Faecal pellets contribution to sinking carbon flux was important, especially at depth where they represented up to 25 % of the total carbon flux. The vertical distribution of different morphotypes of pellets showed a marked pattern with cylindrical faeces (produced by calanoid copepods) present mainly within the euphotic zone, whereas elliptical pellets (produced mainly by smaller copepods) were more abundant at mesopelagic depths. These features, together with the density of matter within the pellets, highlighted the role of the zooplankton community in the transformation of carbon issued from the primary production and the transition of that carbon from the productive surface zone to the Arctic Ocean's interior. Our data indicate that sinking carbon flux in this late summer period is primarily the result of a heterotrophic driven ecosystem as compared to the system driven by autotrophy earlier in the year.

BGD
12, 1247–1283, 2015

1 Introduction

The export of carbon from the surface to the deep ocean via the sinking of particulate organic matter is a major process of the ocean carbon cycle and a key factor in the regulation of the atmospheric CO_2 level (Archer et al., 2000; Siegenthaler et al., 2005). The increase of the latter and the related global warming have become a common subject in climate change research, in which the Arctic Ocean is a privileged target, since it is one of the most vulnerable regions to climate change (Walsh, 2008). Vertical carbon flux in the Arctic Ocean shows multiple facets. There is a marked regional variability illustrated by generally low fluxes in the central Arctic Ocean and high fluxes over the continental shelves and in polynyas (Amiel et al., 2002; Lalande et al., 2009, 2014; Olli et al., 2007). Several factors lead to these different flux scenarios. Over the shelves, the interplay between seasonal ice coverage and break-up, episodical events of wind-driven upwelling and resuspension of sediment seems to be the driving force for highly productive regimes and subsequent elevated fluxes of particulate organic carbon (POC) (Forest et al., 2013; Lalande et al., 2014; Tremblay et al., 2014). Fluxes in the Central Basin are low due to an ineffective "biological pump" (Honjo et al., 2010), as well as to a low primary productivity related to a lack of nutrient supply into the euphotic zone (Lalande et al., 2014).

Annual and seasonal variations are in a first place related to the particular light regime over the Arctic Ocean (Wassmann et al., 2004), the annual light cycle being very regular in contrast to the ice coverage, which is not only irregular with respect to the seasonal break-up in summer but, in the light of global warming, is deemed to disappear at least in parts of this ocean. In the Beaufort Sea, several studies with intercepting sediment traps have shown that the ice-free season is normally the period where maximum fluxes were observed, but they were highly variable within this season between different years (Forest et al., 2007, 2010; Juul-Pedersen et al., 2010). However, high temporal variability was also observed with regard to shelf-basin exchanges, where lateral inputs from nepheloid layers or eddy-driven processes led to flux pulses

BGD
12, 1247–1283, 2015

over the shelf break (Forest et al., 2007) and even beyond the shelf out in the basin (O'Brien et al., 2011). POC flux variability does not only depend on physical but also on biological and chemical parameters, of which the latter have an indirect influence on POC flux through nutrient limited primary production (see above). The main actors of the biotic control of sinking organic particles are on the one hand bacteria, which reduce the flux by decomposition of the particles (Kellogg et al., 2011) and on the other hand grazing zooplankton, primarily copepods in arctic waters, which modulates the flux by the ingestion of phytoplankton and the production of faecal pellets (Wiedmann et al., 2014).

In fact, the different natures of variability in the vertical particle flux are reflected in one of the objectives of the Malina project: to understand the control of biogeochemical fluxes through light penetration and the impact of ongoing climate change on these fluxes. Malina aims at building a self-consistent data set in order to improve our present understanding of biogeochemical fluxes in this remote ocean and the prediction of future changes through modelling. Concerning the vertical particle flux, Forest et al. (2013) estimated POC fluxes over the entire Mackenzie shelf and adjacent areas and explored the spatial variability of these fluxes and its forcing factors. In the present study, our goal is to present a snapshot of the POC fluxes measured in situ along the shelf-break in a more comprehensive manner using a set of parameters obtained from the particulate material. Namely, we aim at documenting the composition of the downward particle flux throughout the water column to highlight the processes that shape its way from the surface to the deep ocean and to identify those, which are most sensitive to forcing factors like sea-ice coverage, upwelling events or zooplankton community structure.

BGD
12, 1247–1283, 2015

2 Material and Methods

2.1 Drifting line deployment and water column survey

Drifting sediment trap moorings were deployed at three sites of the Beaufort Sea during leg 2b of the Malina field campaign in August 2009. The location of the deployment sites is represented in Fig. 1. It shows the sampling grid of the Malina programme and the trap mooring sites within the transects crossing the Mackenzie Shelf. Site 345 had to be moved to the east due to ice coverage at the desired location of the corresponding transect. All three sites are situated on the slope of the Mackenzie shelf in the south-eastern part of the Beaufort Sea, site 135 being the easternmost at the entrance of the Amundsen Gulf. Throughout this article, the three sampling sites will be presented in the order from west to east, i.e. site 345 as the westernmost, site 235 further east and site 135 as the easternmost one.

Figure 2b shows the schematic drawing of the moorings. Each mooring line was equipped with four traps at nominal depths of 40, 85, 150 and 210 m. For each deployment, the length of the mooring line and sampling intervals were adapted to the constraints imposed by bottom depth, ice cover and survey schedules. Detailed information for each trap and mooring deployment is given in Table 1. The traps used were TECHNICAP PPS3/3 of cylindro-conical body shape with an aspect ratio of 2.5 in the cylindrical part and an unbaffled aperture of 0.125 m^{-2}. Particles were collected in 260 mL polyethylene bottles poisoned with a solution of borax buffered formaldehyde 5 % ($v\,v^{-1}$) in filtered (0.2 µm) seawater. The pH was checked after the deployment and immediately before processing the samples in the laboratory.

At all three sites, multiple deployments of a rosette profiler equipped with a conductivity-temperature-depth system (CTD, Seabird SBE-911+), a fluorometer (Seapoint), a transmissometer (Wetlabs C-Star), and a particle camera (Underwater Vision Profiler 5, UVP5 (Picheral et al., 2010)), were conducted in order to document the water column properties before, during and after the drift of the mooring equipped with sediment traps.

BGD
12, 1247–1283, 2015

2.2 Processing and analysis of samples

Upon recovery on board, the sample cups were stored at 4 °C in the dark until they were processed.

Swimmers were handpicked from the samples with forceps under a stereomicroscope. Foraminifera and empty mollusc shells were considered part of the passive sinking flux and hence returned to the main sample.

For the analysis of different parameters, samples were divided into several subsamples. Subsampling was done with a McLane WSD 10 splitting device to obtain two fractions of 1/10 and 4/10 each. Of the latter fractions one was used for mass, POC, nitrogen and thorium-234 and one for pigment analysis, and of the former fractions one for faecal pellet and one for phytoplankton identification.

For mass, POC, N and Th-234 analysis, subsamples were filtered onto a precombusted (500 °C) and pre-weighed micro quartz filter (QMF, ⌀ 25 mm). Filters were then dried in an oven at 50 °C. To determine mass flux the dried filters were transferred to a desiccator cabinet for stabilization at room temperature and then weighed on a Mettler Toledo analytical balance. After weighing, these QMF filters were conditioned for Th-234 measurement through non-destructive counting of the β decay, and that same sample could be used after dismounting, for the analysis of POC. Prior to analysis, inorganic carbon was removed from the sample with a 1 M H_3PO_4 solution in excess, the filters being dried at 50 °C overnight, after each step. POC and N analysis was performed with a "vario EL" elemental analyser (elementar Analysensysteme GmbH) (Miquel et al., 2011).

The subsamples for pigment analysis (fraction 4/10) were filtered onto a precombusted (500 °C) GF/F filter (⌀ 25 mm) and kept frozen at −30 °C. For analysis, residue on these filters was extracted by sonication in 3 mL methanol (100 %) and clarified by filtration through "Whatman" GF/F filters. Extracts were analysed by HPLC diode array detector ("Agilent Technologies" system) the same day. Chromatography was performed on a narrow reversed-phase C8 Zorbax Eclipse XDB column. Pigment

BGD
12, 1247–1283, 2015

detection was obtained at 450, 667 and 770 nm. Vitamin E acetate ("Sigma") was used as internal standard, and external calibration standards were provided by DHI Water and Environment (Denmark). Details on pigment analysis are reported in Ras et al. (2008).

Both faecal pellets and phytoplankton were determined by eye under a stereomicroscope. For faecal pellets, a "Leica MZ 12" stereomicroscope was used. Faecal pellets were counted and sorted into three classes of morphotypes, cylindrical, elliptical and amorphous. Their dimensions were determined with a semi-automated image analysis program, in order to calculate the form-specific volumes and to transform the volumes into organic carbon (Carroll et al., 1998). The determination of phytoplankton species was done according to the Utermöhl method (Utermöhl, 1931).

2.3 Seasonal context from long-term moorings

With the aim of putting the results of the Malina study within a broader context, we obtained a three-year record of vertical POC fluxes (2008–2010) as sampled with long-term sediment traps moored at ca. 100 and 200 m depth in the vicinity of the drifting stations (Fig. 1, Table 2) within the framework of the ArcticNet program. The long-term traps were of the same kind (i.e. TECHNICAP PPS3/3) as those used in the short-term deployment, though the long-term traps were equipped with a 24 instead of a 12 sample cup carrousel. Otherwise, the design of the trap was exactly the same as the one described in Sect. 2.1. Sample cups from long-term traps were filled with filtered seawater (GFF 0.7 µm) adjusted to 35 salinity with NaCl and poisoned with formalin (5 % $v v^{-1}$, sodium borate buffered). Long-term trap samples were processed (i.e. "swimmer" picking, fractioning, filtration), weighed for total mass, acidified and analysed for POC and nitrogen, similarly to short-term trap samples. A full description of the methodology associated with long-term trap samples can be found in Forest et al. (2013).

BGD
12, 1247–1283, 2015

3 Results

3.1 Environmental parameters

The profiles obtained from the hydrographical casts in the vicinity of the trap deployments show the characteristics of the different water masses present in the Beaufort Sea with only minor variations between the three deployment sites (Fig. 2).

As shown in Fig. 2a, salinity values < 31 were measured in the upper 50 m and are typical of the Polar Mixed Layer (PML). Between 50 and 200 m depth the salinity increases from 31 to 34, while the temperature profiles show minimum values. This water mass originates from the Pacific and enters the Arctic Ocean through the Bering Strait into the Chukchi Sea. The fluorescence maxima were mostly found at the top of this water layer around 75 m depth. Transmissivity measured at all three sites did not exhibit any clear pattern, except for generally low values near the surface and an increased variability near the bottom, between profiles at site 135. The waters below 200 m depth are of Atlantic origin and are characterized by the highest salinity (> 34) and a warming of the water temperature compared to the overlying waters.

The mooring configuration is shown in Fig. 2b. Based on the data from the hydrographical casts the trap depths were chosen to monitor (1) the fluxes out of the PML likely to be influenced the most by the inputs from the Mackenzie River, (2) the fluxes out of the layer with highest phytoplankton biomass and production, (3) the fluxes out of the euphotic zone and (4) the fluxes monitored at a depth of other long-term moorings in the area and therefore best comparable with these data. As shown by the profiles (Fig. 2a), recordings at site 135 reached the bottom at around 225 m. The trap at 210 m had to be removed from the mooring line to avoid its grounding.

Based on UVP5 data, the upper water column (< 100 m) at all three sites was particularly devoid of particulate material and aggregates in the range 0.08–10 mm ESD (Fig. 3). We detected a general augmentation in particle inventory within the interval depth of ~ 350 – 500 m at sites 345 and 235, and between ~ 100 – 200 m at site 135 (as seen in the transmissivity signal, Fig. 2). However, the magnitude of those increases

BGD
12, 1247–1283, 2015

varied markedly between each CTD-UVP5 deployment and some profiles did not show any increase at all.

3.2 Flux and composition of settling particles

As explained above, fluxes were recorded at 4 depths down to 210 m at sites 345 and 235, the lowest trap being some 300 m above the bottom. At site 135 only 3 traps were on the mooring line and the lowest at 150 m was around 70 m above ground (Tab. 1).

Mass fluxes measured at the three sites showed different depth patterns (Fig. 4). Although fluxes increased in all cases from the trap at 40 m to the trap below at 85 m, at 150 m depth, mass fluxes were from lowest (15.45 $mg\,m^{-2}\,d^{-1}$ at site 345) to the highest ones (43.20 $mg\,m^{-2}\,d^{-1}$ at site 135) measured at the corresponding sites. Effects of matter resuspension due to the vicinity of the lowest trap to the ocean bottom at site 135 are certainly a possible explanation for the high flux value registered. The overall highest mass fluxes of 54.20 and 51.94 $mg\,m^{-2}\,d^{-1}$ at 85 m of sites 345 and 235 respectively, were observed just below the depth of relatively high phytoplankton biomasses shown by the fluorescence profiles in Fig. 2a.

The vertical distribution of the total carbon fluxes was similar to the mass fluxes, with highest values (15–20 $mg\,m^{-2}\,d^{-1}$) at 85 m and a sharp decrease in flux towards depth, except for site 135 where the trap near to the bottom recorded a relatively high flux of 9.51 $mg\,m^{-2}\,d^{-1}$. At 210 m depth of the two other sites, fluxes were lowest ($< 5\,mg\,m^{-2}\,d^{-1}$).

POC fluxes, too, showed depth distributions very similar to mass and total carbon. This suggests a relationship between mass and carbon fluxes, and that the composition of the biotic compartment of the flux seemed to be similar all over the studied area. Also, the contribution of POC to total carbon was high owing to similar flux values up to 15 $mg\,m^{-2}\,d^{-1}$ for the maximum at 85 m of site 235 and $< 2\,mg\,m^{-2}\,d^{-1}$ at 210 m. Generally, POC fluxes were low with values mostly $< 5\,mg\,m^{-2}\,d^{-1}$. Higher fluxes were observed just below the biomass maximum, and also at 40 m of site 345 and near the bottom of site 135.

BGD
12, 1247–1283, 2015

The flux pattern of inorganic carbon, essentially calcium carbonates, was quite similar to the one of mass flux, but about one order of magnitude lower. As for POC, this shows that the biotic component of the vertical flux was relatively homogeneous over the studied area. The only notable differences concern the results from the deepest traps at sites 345 (210 m) and 135 (150 m), where fluxes were more pronounced compared to the above sampling depths, which is most likely due to the trap's vicinity to the bottom where resuspended matter may have added to the "abiotic" flux. Interestingly, at site 235, where we observed no difference, the deepest trap was the furthest away from the bottom among the moorings at the three sites (Tab. 1).

The composition of the particles collected in the sediment traps (Tab. 3) revealed for almost all the samples a very high content of POC relative to total carbon with values often exceeding 80 or even 90 %. Only at site 235, these values were lower, just slightly below 80 %. But also the POC content relative to the mass flux was rather high. The obtained values were around 25 % for the traps at 40 and 85 m, but decreased to around 10 % in the traps at 210 m of sites 345 and 235.

The inorganic carbon (PIC) being the difference between total and organic carbon, its relative importance was accordingly low at the surface and high at depth. The PIC/POC ratio, in turn, was relatively high in the deep traps (150 and 210 m) except at 150 m of site 345 where very low amounts of PIC were measured.

The C/N ratios did not show big variations within and between the three sites, neither could we observe any clear depth pattern. Ratios between 7 and 8 indicate the presence of phyto- rather than zooplanktonic matter within the sinking flux (Schneider et al., 2003).

3.3 Seasonal and inter-annual variability of downward flux

Using the long-term trap datasets available for the region from 2008–2010 (Table 2), we have created a composite time-series of mean POC fluxes at ~ 100 and ~ 200 m depth (Fig. 5). This figure enables to grasp quickly the seasonality and large variability (i.e. SD) of downward POC fluxes across the eastern Mackenzie Shelf. Over those years,

BGD
12, 1247–1283, 2015

mean POC fluxes oscillated between near-zero values up to $\sim 110\,\mathrm{mg\,C\,m^{-2}\,d^{-1}}$. In general, POC fluxes were higher at 100 than at 200 m depth, except under ice cover during the winter months when the background flux was higher at 200 than at 100 m depth. Peak fluxes (from 1–3 modes) occurred systematically over the summer period, but rapid declines were detected after every of those maxima. In 2009, the peak export flux (as detected at the 4 moorings deployed across the region) was recorded over August, during the month of the Malina campaign. However, the standard deviation associated with the values measured during this period was particularly high (up to ±98 %) at both 100 and 200 m depth.

3.4 Particle characterization

3.4.1 Faecal pellets

The main types of identifiable particles in the sediment trap samples are shown in Fig. 6. Most of these particles were faecal pellets of cylindrical or elliptical form (Fig. 6a–d). A third category that was distinguished contained amorphous pellets. Also, notable numbers of crustacean eggs (Fig. 6e) and foraminifera (Fig. 6f) were observed. Total numbers and the relative importance of the different types of faecal pellets are listed in Table 4. Flux of the total number of pellets showed two distinct vertical patterns. At sites 345 and 135, high numbers were recorded at the surface and in the deepest traps, and at site 235, this pattern was reversed with lowest numbers at surface and bottom. Cylindrical pellets were most important at 40 and 85 m depth at all sites and elliptical ones were present at relatively higher numbers in the deepest traps (150 and 210 m), especially at site 235. Amorphous pellets were generally observed at relatively low numbers and were almost absent at site 135.

The different forms of the faecal pellets were taken into account when calculating their organic carbon content (Carroll et al., 1998). Another outstanding feature was the density of the matter inside the pellet membrane, as illustrated in Fig. 6a–d. Across the sampling sites, there was a clear spatial pattern in the relative importance of fae-

BGD
12, 1247–1283, 2015

cal pellets with different matter density. As an example, the pellets considered as full (highest matter density) were essentially observed at 150 and 200 m depth at all sites. Since the conversion factors for the calculation of the organic content are based on full pellets (Fig. 6a and c) we defined 4 empirical categories of fullness, 100, 75, 50, and 25 %, and corrected the conversion factors accordingly. The resulting flux of organic carbon channelled via faecal pellets is listed in Table 4, which also shows the carbon flux attributed to full (100 %) pellets. While the depth distributions of the pellets' carbon flux resemble the numerical flux with an inverse pattern at site 235 compared to the two other sites, full pellets, were only observed at 150 and 210 m depth. But they represent about 50 to 80 % of the total pellet flux. Overall, the carbon channelled through the flux of faecal pellets represented from a few percent up to 25 % of the total carbon flux, especially in the deepest traps.

3.4.2 Phytoplankton and microzooplankton

A striking feature of the results from the identification of protists in the trap samples was the scarcity of large sized diatoms (e.g. *Chaetoceros* sp., *Thalassiosira* sp.) typical of the polar regions (Coupel et al., 2014; Lovejoy et al., 2002). Among the other diatoms observed, the epiphytic genus *Licmophora* was the most abundant one. Flagellates, especially the dinoflagellate *Pronoctiluca* often showed a high relative importance, and some tintinnids (loricate ciliates) and naked ciliates were important in some traps as e.g. at site 235 (Fig. 7).

Dinoflagellates and the diatom *Licmophora* (85 m) were dominant at site 345, while tintinnids and other ciliates were present at all but one depths but at low relative abundance. At site 235, microzooplankton (dinoflagellates and ciliates) were most abundant and diatoms were relatively important at 40 m depth. Both phytoplankton and microzooplankton were present at site 135, but their absolute abundances were much lower than at the other two sites.

BGD
12, 1247–1283, 2015

3.4.3 Pigment composition

The results of the pigment analysis in the sediment trap samples are presented as concentrations (ng mg^{-1} POC or ppm, Tab. 5). The POC flux being generally low (Fig. 4), many pigments were below detection limits. Only pigments detected in most of the trap samples are presented. One pigment, Peridinin, was observed at all sites but only in the 85 m traps and at 40 m of site 235.

At site 345, highest concentrations were measured for Chl *a* at 85 m depth. The presence of phytoplanktonic material is contrasted by relatively high concentrations of Astaxanthin, which is rather an indicator for zooplankton. These two pigments were the only ones detected in the shallowest trap at 40 m.

The same observations were made at site 235, although the concentrations of the two pigments at 40 m were much higher. In the deeper traps, besides the high Chl *a* concentrations, Fucoxanthin at 150 m and also Prasinoxanthin at 210 m showed relatively high concentrations. The increasing concentrations with depth of Phaeophytin at this site indicate the increase of the relative importance of phytoplankton degradation.

At site 135, Chl *a* was still observed at very high concentrations, but Fucoxanthin was much more abundant than at the other sites and its concentration even increased between 85 and 150 m, which could correspond to the increase in the relative importance of diatoms observed before (see Sect. 3.4.2). Chl *a* was not detected in the trap at 40 m but Astaxanthin, which showed the highest concentration of all three sites at this depth.

3.4.4 Swimmers

Swimmers were abundant in sediment trap samples, particularly at the two shallowest sampling horizons. A dedicated study on the swimmers collected in the sediment traps will be published elsewhere and only a summary is offered here.

Copepods were by far the most abundant group among the swimmers' community. In all traps they represented more than 75 and up to 95 % of the total abundance.

BGD
12, 1247–1283, 2015

Among the other groups, only appendicularians (mostly *Oikopleura* spp.) and pelagic molluscs (essentially *Limacina helicina*) were observed at notable numbers. The relative depth distribution of the different organisms was similar at all sites. In the shallow traps (40 m), a herbivorous copepod (*Calanus glacialis*) and appendicularians (*Oikopleura* spp.) represented 40 to 70 % of all swimmers present. In the traps below the phytoplankton biomass maximum at 85 m, the absolute numbers of swimmers were about twice as much as those from 40 m depth, and the omnivorous copepod *Metridia longa* was by far the most abundant swimmer organism (60–75 %). Among the other organisms found at 85 m depth, the herbivorous pteropod *Limacina helicina* was present at all sites. In the deepest traps at 150 m (all sites) and 210 m (sites 345 and 235) the absolute numbers of swimmers decreased five to ten fold relative to the shallower traps. The omnivorous *Metridia longa* became even more important, but the carnivorous copepod *Pareuchaeta glacialis* represented 15–25 % of the swimmers at 150 m depth of sites 235 and 135. This copepod was also present in all other traps at percentages between 10 and 15 %, except at site 345 where it was absent at 150 m and represented 25 % at 85 m. The only herbivore swimmers observed in these deepest traps were *Limacina helicina* (150 m, sites 235 and 135) and *Calanus hyperboreus* (150 and 210 m, site 235).

4 Discussion

Sediment trap moorings anchored at the ocean floor on a long-term basis have a relatively long history in arctic research (Honjo et al., 2008 and refs. herein). However, the deployment of drifting sediment trap moorings in the Beaufort Sea was part of only a few oceanographic expeditions. This is most likely due to the ice conditions not favourable to such deployments during most of the year and over a vast area. An indirect method based on the deficit between the particle reactive Th-234 and its conservative parent radionuclide U-238 (Rutgers van der Loeff et al., 2006) is better adapted

BGD
12, 1247–1283, 2015

to these conditions and was used in various studies to assess the vertical POC flux in the Arctic seas (Wassmann et al., 2004).

When comparing our results with the published data from the same region and at similar depths, we notice that the POC fluxes we measured were always at the lower end of the broad range of fluxes reported, which spans from some 10 mg C m^{-2} d^{-1} to a few hundred mg of carbon per m^2 and per day. Such was the case for the studies using drifting trap moorings (Juul-Pedersen et al., 2010; Lalande et al., 2007; Sallon et al., 2011) as well as for the ones obtained via the $^{234}Th/^{238}U$ disequilibrium (Baskaran et al., 2003; Lalande et al., 2007; Moran and Smith, 2000).

Annual and seasonal variabilities and also spatial heterogeneities may be at the origin of the flux differences between the present study and the published data. Moreover, the traps of our drifting mooring (collecting surface: 0.125 m^2) were rather large compared to the above mentioned studies (collecting surface: < 0.03 m^2). Sediment traps of this former type, however, are part of fixed moorings that have been deployed in the framework of the ArcticNet programme, and which were moored in the vicinity of our deployments during the Malina campaign (Tab. 2).

Compared to the POC fluxes recorded by these traps (Fig. 5), the present fluxes were still relatively low. But as we already mentioned, the data are shown as a composite figure and the standard deviation is particularly high during the peak flux periods. These data have been presented and discussed in more detail elsewhere (Forest et al., 2013) and recalled us the fact that such peak events happen at short time scales relative to the long time series. With respect to our data, we consider that, although the late summer months seem to be a period of an elevated flux regime (Forest et al., 2013), the vertical particle flux monitored by our traps during < 3 days is situated between two peak events. From the data recorded by the particle camera (UVP5) we know at least that at that time, the particle load of the water column along the drifting path was very low (Fig. 3).

If the flux quantity is an important factor of carbon cycling in terms of e.g. parameterization and validation of models, the flux quality is as important when it comes to

BGD
12, 1247–1283, 2015

conceptualization of models (Le Fouest et al., 2013). The composition of the particulate matter collected in our sediment traps is characterized by both a relatively high total carbon content (average 26 ± 7 %) and a high C_{org} to C_{tot} ratio. This indicates that an important part of the settling particles is of biogenic origin and that these particles contain relatively small amounts of calcium carbonates. It also explains that highest fluxes were observed just below the depth layer of maximum phytoplankton biomass (Figs. 2 and 4) and underlines that the decrease at depth of the organic carbon content in the particles settling further down the water column is due to remineralisation (Tab. 3). However, these results suggest that the Mackenzie River plume seems to have little or no influence on the particle composition at the drifting trap locations. Surface POC concentrations obtained through satellite image processing from the sampling period confirm this observation (Forest et al., 2013).

Faecal pellets form a well distinct part of the sinking particles and have been reported to represent sometimes their major part in the Beaufort Sea area (Forest et al., 2008; Juul-Pedersen et al., 2010). The quantitative distributions of pellets in the present study, be it numerically or in terms of carbon, indicate at sites 345 and 135 relatively high grazing activities above the trap at 40 m depth and above the deepest trap at 210 m (Tab. 4). Lowest quantities of pellets were observed in the samples from 85 m just below the phytoplankton biomass maximum. This is in contrast to the findings by Forest et al. (2012), who found good agreement between maximum phytoplankton abundance and copepods, which were by far the most abundant grazers around 60 m depth. It follows that, either grazing activity at this depth was low despite the relatively high food availability, or defecation from these grazers took place above the 40 m depth horizon. A detailed study on copepod migration in the Beaufort Sea (Darnis and Fortier, 2014) did not show evidence of diel but rather seasonal vertical migration, which does not explain an eventual short-term displacement observed in our study. However, Cottier et al. (2006) describe an unsynchronized migration by large calanoid copepods, which took place at around the same period of the year in an arctic fjord. We do not have data to confirm such behaviour. However, our data showed that at 40 m the pellet

BGD
12, 1247–1283, 2015

fluxes were highly variable across the 3 sites, but were much less variable at 85 m. We therefore do not exclude the possibility that the depth distributions at sites 345 and 135 are due to this high variability observed at 40 m. Nonetheless, the pellet flux did not have a considerable impact on the total carbon flux distribution in the euphotic zone, since it represented < 10 %, except at 40 m of site 135, where a lower pellet flux would accentuate the discrepancy of the carbon flux between 40 and 85 m depth.

The increase of the faecal pellet flux at depth can best be explained by the qualitative features of the faecal particles. The relative contribution of the two major morphotypes, cylindrical and elliptical pellets, was high in the two upper traps for the former and in the lower traps for the latter ones, or in other words, the vertical flux patterns of these morphotypes were inversed. This implies on the one hand, that cylindrical pellets are less produced at greater depths and that the sinking pellets from the upper layers are degraded and remineralized before reaching these depths (Honjo et al., 2010), and on the other hand, that there is a production of elliptical pellets below the trap at 85 m and/or that elliptical pellets produced above are more refractory than cylindrical ones and are therefore sampled by the traps at greater depths.

Cylindrical pellets are mainly produced by large calanoid copepods (Carroll et al., 1998; Yoon et al., 2001), which were indeed the most abundant zooplankton observed in surface waters at this period of the year in the Beaufort Sea (Forest et al., 2012), but also elsewhere in the Arctic Ocean (Daase et al., 2008; Kosobokova and Hirche, 2000; Kosobokova and Hopcroft, 2010; Thor et al., 2005). The smaller elliptical faecal pellets are attributed to small copepods, but also to appendicularians (Carroll et al., 1998; Yoon et al., 2001). Forest et al. (2012) reported a small copepod genus, *Oncaea* spp., as one of the most abundant copepods in the study area, and which represented around 80 % in the size class < 1 mm (equivalent spherical diameter) of the zooplankton assemblage caught by a plankton net. Also, *Oncaea* is well known to dwell in and to be adapted to the meso- and bathypelagic zone below the euphotic layer (Kosobokova and Hopcroft, 2010; Thor et al., 2005). These copepods were most likely the main producers of faecal pellets intercepted by our deep sediment traps. The depth distribution

BGD
12, 1247–1283, 2015

of the swimmers in our traps corroborates these findings, though not quantitatively but with respect to the planktonic feeding regimes. Large herbivore copepods (*Calanus gracilis*) and appendicularians were the main swimmers in the trap at 40 m; a typically omnivorous copepod species (*Metridia longa*) prevailed in the intermediate traps, and in the deepest traps a carnivorous species (*Paraeuchaeta glacialis*) was most abundant after *M. longa*. These copepods do not produce elliptical but cylindrical pellets, but their feeding regime, especially that of *M. longa*, is the same as that of the *Oncaea* species. Whatever the reason is why these small copepods were virtually absent as swimmers, we still believe that given the trophic conditions, *Oncaea* were mainly producing the elliptical pellets we observed in the deep traps.

An even stronger evidence for the above scenario comes from the density level of the matter packed inside the faecal pellet membrane. Our data revealed a clear pattern for both morphotypes, with rather low density pellets at the surface and high density pellets at depth. Pellets within the 100 % fullness category (see Sect. 3.4.1) were almost exclusively elliptical pellets, and they were only observed in the samples of the deepest traps. Feinberg et al. (1998) found in a feeding experiment with *Acartia tonsa*, that feeding on phytoplanktonic matter yielded pellets with low density, whereas feeding on heterotrophic matter resulted in a density increase of the pellets. Although we do not have experimental data from the copepod species present during our study, we can assume that the distribution pattern of the different categories of fullness reflected the trophic condition at each of the mooring locations. Within the euphotic zone, large calanoid copepods but also larvaceans are grazing upon the biomass issued from the primary production and consisting of photosynthetic flagellates and diatoms, as shown in our data from the microscopic investigation of the sinking material (cf. Fig. 7), and as reported by a pigment study in the same area (Coupel et al., 2014). Such food yields relatively low density faecal pellets, which undergo bacterial degradation along their vertical sinking path, but also serve as a potential food source to the deeper-dwelling zooplankton community characterized by an omnivorous feeding behaviour. Although these pellets represent less than a third of the particle flux arriving in this zone, they are

BGD
12, 1247–1283, 2015

certainly part of the material described as a "fluffy and sticky gel-like matrix" by Forest et al. (2013) and composed among others, of ciliates and dinoflagellates (Fig. 7), which yields rather dense faecal pellets (Feinberg and Dam, 1998).

As a summary, the vertical particle flux measured within the shelf-basin area of the eastern Beaufort Sea during the late summer period of the 2009 Malina field campaign is at the lower end of fluxes registered in this area. However, similar or even lower fluxes have been reported from elsewhere in the Arctic Ocean (Cai et al., 2010; Chen et al., 2003). Compared to the long-term series data obtained from ArcticNet fixed moorings deployed in the vicinity, the fluxes from this study could be identified as background level flux, at least for the period 2008–2010 (Fig. 5). Although late August 2009 was a period of elevated fluxes for that year, the high spatial and also temporal variability of particle fluxes (cf. Forest et al., 2013) does not exclude short periods of minimal flux. Extrapolation of short-term data should be done with much precaution, but situated within long-term series, such data sets can provide valuable information on processes that govern the fluxes under the given conditions. Integrated field studies such as the ArcticNet-Malina field campaign are an ideal platform to monitor these conditions. A rather complete set of complementary parameters measured on the sinking particles together with other data from the Malina study allowed us to analyse some processes involved in the export of particulate carbon from the surface to the deep ocean. In particular, we could highlight (1) the role of zooplankton, especially copepods, in the transformation of assimilated carbon by phytoplankton into particular organic carbon and (2) the transition of that carbon from the euphotic zone to the mesopelagic zone where it is re-processed by another zooplankton community. These processes are closely linked to the trophic structure within the pelagic food web and vary accordingly. Yet, we believe that they are also active during peak flux periods, since, as already mentioned by Forest et al. (2013), "the sinking POC can be viewed as what heterotrophic plankton were not able to assimilate". This shows the need not only for both short- and long-term surveys but also for an understanding of the mechanisms that lead to the transition between high and low fluxes (e.g. Andersen and Prieur,

BGD
12, 1247–1283, 2015

2000), for which abiotic rather than biotic factors seem to be of primordial importance (Watanabe et al., 2014). Surely, in order to predict POC fluxes within a complex ecosystem such as the Arctic Ocean, all of physical, chemical and biological parameters are necessary to conceptualize and parameterize reliable models.

Acknowledgements. The International Atomic Energy Agency is grateful to the Government of the Principality of Monaco for the support provided to its Environment Laboratories. This study was conducted as part of the Malina Scientific Programme funded by ANR (Agence Nationale de la Recherche), INSU-CNRS (Institut National des Sciences de l'Univers – Centre National de la Recherche Scientifique) and CNES (Centre National d'Etudes Spatiales) from France, and ESA (European Space Agency). Additional support from ArcticNet (a Network of Centres of Excellence of Canada) was welcomed and appreciated. We thank the captain and crew of the Canadian Coast Guard research vessel *Amundsen* for their assistance at sea. We are particularly indebted to Nicolas Evensen (faecal pellets), Josephine Ras (pigments), Fernando Gomez (phytoplankton identification), Makoto Sampei (trap analyses) and Cyril Aubry (swimmers identification) for their laboratory contribution. Special thanks to Marc Picheral and Lars Stemmann for the processing of UVP data, and to Pascal Guillot for QA/QC of CTD profiles.

References

Amiel, D., Cochran, J. K., and Hirschberg, D. J.: Th-234/U-238 disequilibrium as an indicator of the seasonal export flux of particulate organic carbon in the North Water, Deep-Sea Res. Part II: Top. Stud. Oceanogr., 49, 5191–5209, 2002.

Andersen, V. and Prieur, L.: One-month study in the open NW Mediterranean Sea (DYNAPROC experiment, May 1995): overview of the hydrobiogeochemical structures and effects of wind events, Deep-Sea Res. Part I: Oceanogr. Res. Pap., 47, 397–422, 2000.

Archer, D., Winguth, A., Lea, D., and Mahowald, N.: What caused the glacial/interglacial atmospheric pCO_2 cycles?, Rev. Geophys., 38, 159–189, doi:10.1029/1999rg000066, 2000.

Baskaran, M., Swarzenski, P. W., and Porcelli, D.: Role of colloidal material in the removal of Th-234 in the Canada Basin of the Arctic Ocean, Deep-Sea Res. Part I-Oceanogr. Res. Pap., 50, 1353–1373, 2003.

BGD
12, 1247–1283, 2015

Cai, P., van der Loeff, M. R., Stimac, I., Noethig, E. M., Lepore, K., and Moran, S. B.: Low export flux of particulate organic carbon in the central Arctic Ocean as revealed by (234)Th : (238)U disequilibrium, J. Geophys. Res.-Oceans, 115, C10037, doi:10.1029/2009jc005595, 2010.

Carroll, M. L., Miquel, J. C., and Fowler, S. W.: Seasonal patterns and depth-specific trends of zooplankton fecal pellet fluxes in the northwestern Mediterranean Sea, Deep-Sea Res. Part I-Oceanogr. Res. Pap., 45, 1303–1318, 1998.

Chen, M., Huang, Y. P., Cai, P. G., and Guo, L. D.: Particulate organic carbon export fluxes in the Canada Basin and Bering Sea as derived from Th-234/U-238 disequilibria, Arctic, 56, 32–44, 2003.

Cottier, F. R., Tarling, G. A., Wold, A., and Falk-Petersen, S.: Unsynchronized and synchronized vertical migration of zooplankton in a high arctic fjord, Limnol. Oceanogr., 51, 2586–2599, 2006.

Coupel, P., Matsuoka, A., Ruiz-Pino, D., Gosselin, M., Claustre, H., Marie, D., Tremblay, J.-É., and Babin, M.: Pigment signatures of phytoplankton communities in the Beaufort Sea, Biogeosciences Discuss., 11, 14489–14530, doi:10.5194/bgd-11-14489-2014, 2014.

Daase, M., Eiane, K., Aksnes, D. L., and Vogedes, D.: Vertical distribution of *Calanus* spp., and *Metridia longa* at four Arctic locations, Mar. Biol., 4, 193–207, 2008.

Darnis, G. and Fortier, L.: Temperature, food and the seasonal vertical migration of key arctic copepods in the thermally stratified Amundsen Gulf (Beaufort Sea, Arctic Ocean), J. Plankton Res., 36, 1092–1108, doi:10.1093/plankt/fbu035, 2014.

Feinberg, L. R. and Dam, H. G.: Effects of diet on dimensions, density and sinking rates of fecal pellets of the copepod *Acartia tonsa*, Mar. Ecol.-Prog. Ser., 175, 87–96, 1998.

Forest, A., Sampei, M., Hattori, H., Makabe, R., Sasaki, H., Fukuchi, M., Wassmann, P., and Fortier, L.: Particulate organic carbon fluxes on the slope of the Mackenzie Shelf (Beaufort Sea): physical and biological forcing of shelf-basin exchanges, J. Marine Syst., 68, 39–54, doi:10.1016/j.jmarsys.2006.10.008, 2007.

Forest, A., Sampei, M., Makabe, R., Sasaki, H., Barber, D. G., Gratton, Y., Wassmann, P., and Fortier, L.: The annual cycle of particulate organic carbon export in Franklin Bay (Canadian Arctic): environmental control and food web implications, J. Geophys. Res.-Oceans 113, C03s05, doi:10.1029/2007jc004262, 2008.

Forest, A., Belanger, S., Sampei, M., Sasaki, H., Lalande, C., and Fortier, L.: Three-year assessment of particulate organic carbon fluxes in Amundsen Gulf (Beaufort Sea): satellite

BGD
12, 1247–1283, 2015

observations and sediment trap measurements, Deep-Sea Res. Part I-Oceanogr. Res. Pap., 57, 125–142, doi:10.1016/j.dsr.2009.10.002, 2010.
Forest, A., Stemmann, L., Picheral, M., Burdorf, L., Robert, D., Fortier, L., and Babin, M.: Size distribution of particles and zooplankton across the shelf-basin system in southeast Beaufort Sea: combined results from an Underwater Vision Profiler and vertical net tows, Biogeosciences, 9, 1301–1320, doi:10.5194/bg-9-1301-2012, 2012.
Forest, A., Babin, M., Stemmann, L., Picheral, M., Sampei, M., Fortier, L., Gratton, Y., Bélanger, S., Devred, E., Sahlin, J., Doxaran, D., Joux, F., Ortega-Retuerta, E., Martín, J., Jeffrey, W. H., Gasser, B., and Carlos Miquel, J.: Ecosystem function and particle flux dynamics across the Mackenzie Shelf (Beaufort Sea, Arctic Ocean): an integrative analysis of spatial variability and biophysical forcings, Biogeosciences, 10, 2833–2866, doi:10.5194/bg-10-2833-2013, 2013.
Honjo, S., Manganini, S. J., Krishfield, R. A., and Francois, R.: Particulate organic carbon fluxes to the ocean interior and factors controlling the biological pump: a synthesis of global sediment trap programs since 1983, Prog. Oceanogr., 76, 217–285, doi:10.1016/j.pocean.2007.11.003, 2008.
Honjo, S., Krishfield, R. A., Eglinton, T. I., Manganini, S. J., Kemp, J. N., Doherty, K., Hwang, J., McKee, T. K., and Takizawa, T.: Biological pump processes in the cryopelagic and hemipelagic Arctic Ocean: Canada Basin and Chukchi Rise, Prog. Oceanogr., 85, 137–170, doi:10.1016/j.pocean.2010.02.009, 2010.
Juul-Pedersen, T., Michel, C., and Gosselin, M.: Sinking export of particulate organic material from the euphotic zone in the eastern Beaufort Sea, Marine Ecology-Progress Series, 410, 55–70, doi:10.3354/meps08608, 2010.
Kellogg, C. T. E., Carpenter, S. D., Renfro, A. A., Sallon, A., Michel, C., Cochran, J. K., and Deming, J. W.: Evidence for microbial attenuation of particle flux in the Amundsen Gulf and Beaufort Sea: elevated hydrolytic enzyme activity on sinking aggregates, Polar Biol., 34, 2007–2023, doi:10.1007/s00300-011-1015-0, 2011.
Kosobokova, K. and Hirche, H. J.: Zooplankton distribution across the Lomonosov Ridge, Arctic Ocean: species inventory, biomass and vertical structure, Deep-Sea Res. Part I-Oceanogr. Res. Pap., 47, 2029–2060, 2000.
Kosobokova, K. N. and Hopcroft, R. R.: Diversity and vertical distribution of mesozooplankton in the Arctic's Canada Basin, Deep-Sea Res. Part II-Top. Stud. Oceanogr., 57, 96–110, 2010.

BGD
12, 1247–1283, 2015

Lalande, C., Lepore, K., Cooper, L. W., Grebmeier, J. M., and Moran, S. B.: Export fluxes of particulate organic carbon in the Chukchi Sea: a comparative study using Th-234/U-238 disequilibria and drifting sediment traps, Mar. Chem., 103, 185–196, 2007.

Lalande, C., Forest, A., Barber, D. G., Gratton, Y., and Fortier, L.: Variability in the annual cycle of vertical particulate organic carbon export on Arctic shelves: contrasting the Laptev Sea, Northern Baffin Bay and the Beaufort Sea, Cont. Shelf Res., 29, 2157–2165, doi:10.1016/j.csr.2009.08.009, 2009.

Lalande, C., Noethig, E.-M., Somavilla, R., Bauerfeind, E., Shevchenko, V., and Okolodkov, Y.: Variability in under-ice export fluxes of biogenic matter in the Arctic Ocean, Global Biogeochem. Cy., 28, 571–583, 2014.

Le Fouest, V., Zakardjian, B., Xie, H., Raimbault, P., Joux, F., and Babin, M.: Modeling plankton ecosystem functioning and nitrogen fluxes in the oligotrophic waters of the Beaufort Sea, Arctic Ocean: a focus on light-driven processes, Biogeosciences, 10, 4785–4800, doi:10.5194/bg-10-4785-2013, 2013.

Lovejoy, C., Legendre, L., Martineau, M.-J., Bâcle, J., and von Quillfeldt, C. H.: Distribution of phytoplankton and other protists in the North Water, Deep-Sea Res. Pt. II, 49, 5027–5047, doi:10.1016/S0967-0645(02)00176-5, 2002.

Miquel, J.-C., Martin, J., Gasser, B., Rodriguez y Baena, A., Toubal, T., and Fowler, S. W.: Dynamics of particle flux and carbon export in the northwestern Mediterranean Sea: A two decade time-series study at the DYFAMED site, Prog. Oceanogr., 91, 461–481, 2011.

Moran, S. B. and Smith, J. N.: Th-234 as a tracer of scavenging and particle export in the Beaufort Sea, Cont. Shelf Res., 20, 153–167, doi:10.1016/s0278-4343(99)00065-5, 2000.

O'Brien, M. C., Melling, H., Pedersen, T. F., and Macdonald, R. W.: The role of eddies and energetic ocean phenomena in the transport of sediment from shelf to basin in the Arctic, J. Geophys. Res.-Oceans 116, C08001, doi:10.1029/2010jc006890, 2011.

Olli, K., Wassmann, P., Reigstad, M., Ratkova, T. N., Arashkevich, E., Pasternak, A., Matrai, P. A., Knulst, J., Tranvik, L., Klais, R., and Jacobsen, A.: The fate of production in the central Arctic Ocean – Top-down regulation by zooplankton expatriates?, Prog. Oceanogr., 72, 84–113, 2007.

Picheral, M., Guidi, L., Stemmann, L., Karl, D. M., Iddaoud, G., and Gorsky, G.: The Underwater Vision Profiler 5: an advanced instrument for high spatial resolution studies of particle size spectra and zooplankton, Limnol. Oceanogr. Methods, 8, 462–473, 2010.

BGD
12, 1247–1283, 2015

Ras, J., Claustre, H., and Uitz, J.: Spatial variability of phytoplankton pigment distributions in the Subtropical South Pacific Ocean: comparison between in situ and predicted data, Biogeosciences, 5, 353–369, doi:10.5194/bg-5-353-2008, 2008.

Rutgers van der Loeff, M. M., Sarin, M. M., Baskaran, M., Benitez-Nelson, C. R., Buesseler, K. O., Charette, M. A., Dai, M., Gustafsson, O., Masque, P., Morris, P. J., Orlandini, K., Rodriguez y Baena, A. M., Savoye, N., Schmidt, S., Turnewitsch, R., Voge, I., and Waples, J. T.: A review of present techniques and methodological advances in analyzing Th-234 in aquatic systems, Mar. Chem., 100, 190–212, 2006.

Sallon, A., Michel, C., and Gosselin, M.: Summertime primary production and carbon export in the southeastern Beaufort Sea during the low ice year of 2008, Polar Biol. 34, 1989–2005, doi:10.1007/s00300-011-1055-5, 2011.

Schneider, B., Schlitzer, R., Fischer, G., and Nothig, E. M.: Depth-dependent elemental compositions of particulate organic matter (POM) in the ocean, Global Biogeochem. Cy., 17, 1032, doi:10.1029/2002GB001871, 2003.

Siegenthaler, U., Stocker, T. F., Monnin, E., Lüthi, D., Schwander, J., Stauffer, B., Raynaud, D., Barnola, J.-M., Fischer, H., Masson-Delmotte, V., and Jouzel, J.: Stable Carbon Cycle–Climate Relationship During the Late Pleistocene, Science, 310, 1313–1317, doi:10.1126/science.1120130, 2005.

Thor, P., Nielsen, T. G., Tiselius, P., Juul-Pedersen, T., Michel, C., Moller, E. F., Dahl, K., Selander, E., and Gooding, S.: Post-spring bloom community structure of pelagic copepods in the Disko Bay, Western Greenland, J. Plankton Res., 27, 341–356, 2005.

Tremblay, J.-É., Raimbault, P., Garcia, N., Lansard, B., Babin, M., and Gagnon, J.: Impact of river discharge, upwelling and vertical mixing on the nutrient loading and productivity of the Canadian Beaufort Shelf, Biogeosciences, 11, 4853–4868, doi:10.5194/bg-11-4853-2014, 2014.

Utermöhl, H.: Neue Wege in der quantitativen Erfassung des Planktons (mit besonderer Berücksichtigung des Ultraplanktons). Verhandlungen der Internationalen Vereinigung für Theoretische und Angewandte Limnologie, 5, 567–596, 1931.

Walsh, J. E.: Climate of the Arctic marine environment, Ecol. Appl., 18, S3–S22, 2008.

Wassmann, P., Bauerfeind, E., Fortier, M., Fukuchi, M., Hargrave, B., Moran, B., Noji, T., Nöthig, E. M., Olli, K., Peinert, R., Sasaki, H., and Shevchenko, V.: Particulate organic carbon flux to the Arctic Ocean sea floor, in: Organic Carbon Cycle in the Arctic Ocean, edited by: Stein, R. and MacDonald, R. W., Springer, Berlin Heidelberg, 101–138, 2004.

BGD
12, 1247–1283, 2015

Watanabe, E., Onodera, J., Harada, N., Honda, M. C., Kimoto, K., Kikuchi, T., Nishino, S., Matsuno, K., Yamaguchi, A., Ishida, A., and Kishi, M. J.: Enhanced role of eddies in the Arctic marine biological pump, Nature Communications, 5, 3950, doi:10.1038/ncomms4950, 2014.

Wiedmann, I., Reigstad, M., Sundfjord, A., and Basedow, S.: Potential drivers of sinking particle's size spectra and vertical flux of particulate organic carbon (POC): turbulence, phytoplankton, and zooplankton, J. Geophys. Res.-Oceans, 119, 6900–6917, doi:10.1002/2013jc009754, 2014.

Yoon, W. D., Kim, S. K., and Han, K. N.: Morphology and sinking velocities of fecal pellets of copepod, molluscan, euphausiid, and salp taxa in the northeastern tropical Atlantic, Mar. Biol., 139, 923–928, 2001.

BGD
12, 1247–1283, 2015

Table 1. Drifting line deployment specifications.

Sampling stations	345	235	135
Deployment depths (m)	38, 85, 152, 211	38, 83, 151, 210	39, 87, 154
Bottom depth (m)*	500–600	550–650	220–230
Deployment date (UTC)	14 Aug 2009	22 Aug 2009	20 Aug 2009
Retrieval date (UTC)	16 Aug 2009	24 Aug 2009	22 Aug 2009
Deployment location	71.330° N 132.556° W	71.775° N 130.726° W	71.321° N 127.495° W
Retrieval location	71.390° N 132.649° W	71.713° N 130.797° W	71.213° N 127.344° W
Sampling duration (h)	32	50	28

* Indicates depth range within drifting track.

BGD
12, 1247–1283, 2015

Table 2. Sampling period and location of long-term sediment traps used to document the seasonal and inter-annual variability (2008–2010) of downward particle fluxes in the vicinity of the drifting stations.

Mooring	Sampling starts	Sampling ends	Latitude (° N)	Longitude (° W)	Sampling depth(s)
CA08	21 Oct 2007	24 Jul 2008	71.0539	126.0227	104 m
CA16	01 Nov 2007	28 Jul 2008	71.7904	126.4929	112 and 213 m
CA05	27 Jul 2008	31 Aug 2009	71.3125	127.5824	108 m
CA16	29 Jul 2008	31 Aug 2009	71.7868	126.4970	110 and 211 m
A1	21 Jul 2009	25 Jun 2010	70.7617	136.0083	98 and 199 m
G09	24 Jul 2009	29 Jun 2010	71.0025	135.4793	100 and 201 m
CA16	13 Oct 2009	16 Oct 2010	71.8015	126.5170	103 and 204 m
A1	13 Sep 2010	31 Aug 2011	70.7622	136.0094	101 and 201 m

BGD
12, 1247–1283, 2015

Table 3. Mass flux (DW) and composition of sedimenting particles.

Sampling stations	345				235				135		
Sampling depths (m)	40	85	150	210	40	85	150	210	40	85	150
Mass flux ($mg\,m^{-2}\,d^{-1}$)	45	54	15	21	15	52	27	11	20	31	43
Tot. carbon (TC) (% of DW)	31	28	29	19	31	38	25	14	18	31	22
Org. carbon (% of DW)	27	23	27	11	27	29	18	10	17	28	18
Inorg. Carbon (% of DW)	4.1	5.0	1.8	7.7	4.6	8.3	6.9	3.5	1.2	2.1	4.0
Org. carbon (% of TC)	87	82	94	59	85	78	73	74	94	93	82
Nitrogen (% of DW)	5.6	2.8	4.5	1.9	5.0	4.7	4.1	1.6	2.3	4.5	2.9
C : N atomic	5.7	9.3	7.1	7.0	6.2	7.3	5.2	7.4	8.7	7.4	7.3
$C_{inorg} : C_{org}$	0.15	0.22	0.06	0.69	0.17	0.28	0.37	0.35	0.07	0.07	0.22

BGD
12, 1247–1283, 2015

Table 4. Faecal pellet flux (numerical and carbon) and relative contribution of each type of pellets to the total numerical flux. Note: different units for pellet flux (mg and µg).

Sampling stations	345				235				135		
Sampling depths (m)	40	85	150	210	40	85	150	210	40	85	150
Pellet flux (all pellets) (mg C_{org} m^{-2} d^{-1})	1.32	0.45	0.77	0.92	0.22	0.34	0.44	0.27	0.66	0.25	0.82
Pellet flux (only 100 % full pellets) (µg C_{org} m^{-2} d^{-1})	17.4	7.6	439.8	670.0	0.0	2.7	362.3	220.4	0.7	0.0	424.2
Numerical flux (all pellets) (nb. m^{-2} d^{-1})	4680	2880	1920	3120	806	2342	2458	960	4389	2057	4663
Cylindrical pellets (%)	56.4	52.1	18.8	11.5	52.4	62.3	9.4	20.0	85.9	53.3	22.1
Elliptical pellets (%)	32.1	35.4	56.3	40.4	47.6	32.8	76.6	60.0	14.1	46.7	69.1
Amorphous pellets (%)	11.5	12.5	25.0	48.1	0.0	4.9	14.1	20.0	0.0	0.0	8.8

BGD
12, 1247–1283, 2015

Table 5. Concentration of major pigments in sedimenting particles at the 3 mooring sites (in ng mg^{-1} POC).

Sampling stations		345	235	135
40 m:	Total Chl *a*	5.6	76.3	n.d.
	Astaxanthin	7.8	87.1	138.3
85 m:	Total Chl *a*	185.5	393.4	562.8
	Total Chl *b*	26.7	61.4	42.2
	Fucoxanthin	35.5	36.0	179.6
	Prasinoxanthin	26.4	52.4	42.7
	Astaxanthin	66.4	72.1	n.d.
	Phaeophytin *a*	15.3	13.4	23.1
150 m:	Total Chl *a*	–	303.2	432.2
	Total Chl *b*	–	32.7	42.7
	Fucoxanthin	–	86.9	182.8
	Prasinoxanthin	–	26.6	46.5
	Astaxanthin	–	23.5	n.d
	Phaeophytin *a*	–	24.9	26.9
210 m:	Total Chl *a*	n.d.	405.9	–
	Total Chl *b*	n.d.	62.7	–
	Fucoxanthin	n.d.	67.9	–
	Prasinoxanthin	n.d.	80.1	–
	Astaxanthin	n.d.	29.6	–
	Phaeophytin *a*	n.d.	43.5	–

n.d. = not detected (below detection limit); – = not sampled or measured.

BGD
12, 1247–1283, 2015

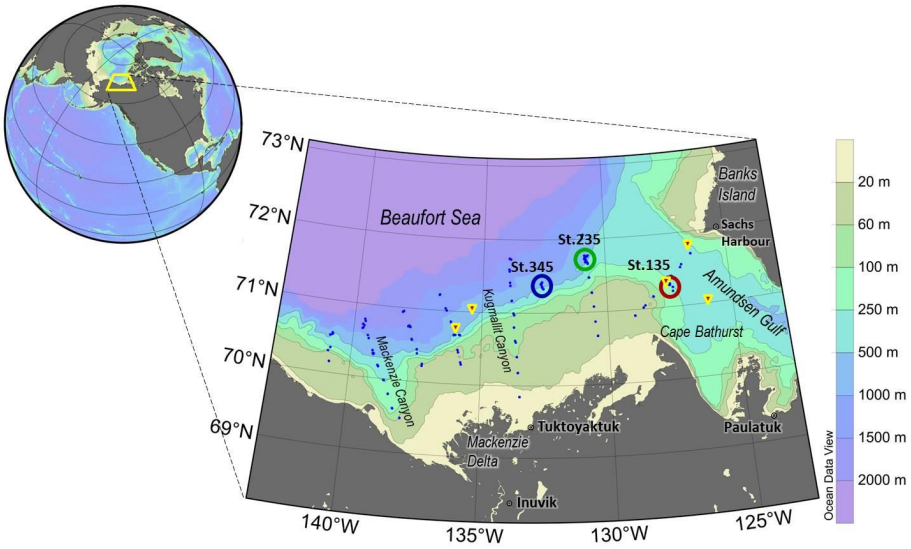

Figure 1. Map of the region and close-up on sampling area; blue, green and red circles represent areas of drifting trap deployment and yellow triangles sites of long-term moorings. Blue dots depict main CTD stations of the Malina programme sampling grid. Drifting trap sampling was limited to the eastern part of the area because of the sea-ice cover during the first part of the cruise.

BGD
12, 1247–1283, 2015

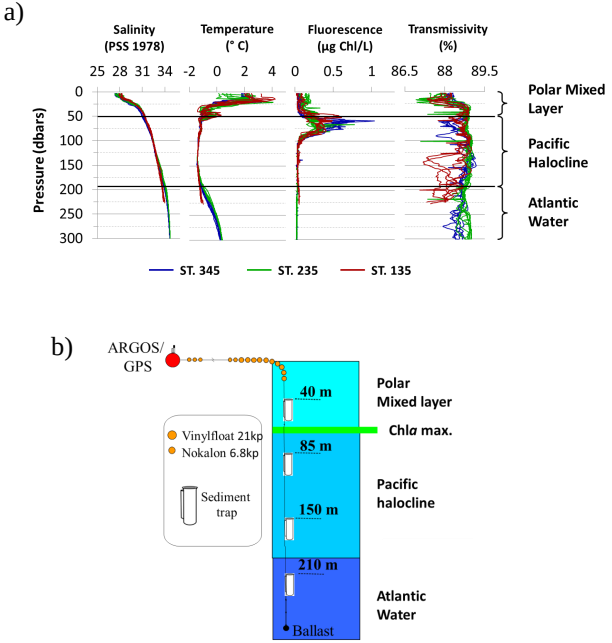

Figure 2. Environmental and mooring parameters: **(a)** vertical profiles of salinity, temperature, fluorescence and transmissivity and main water masses at the three sites of drifting trap deployment; **(b)** mooring configuration including sediment trap depths and horizon of maximum chloropyll *a*.

BGD
12, 1247–1283, 2015

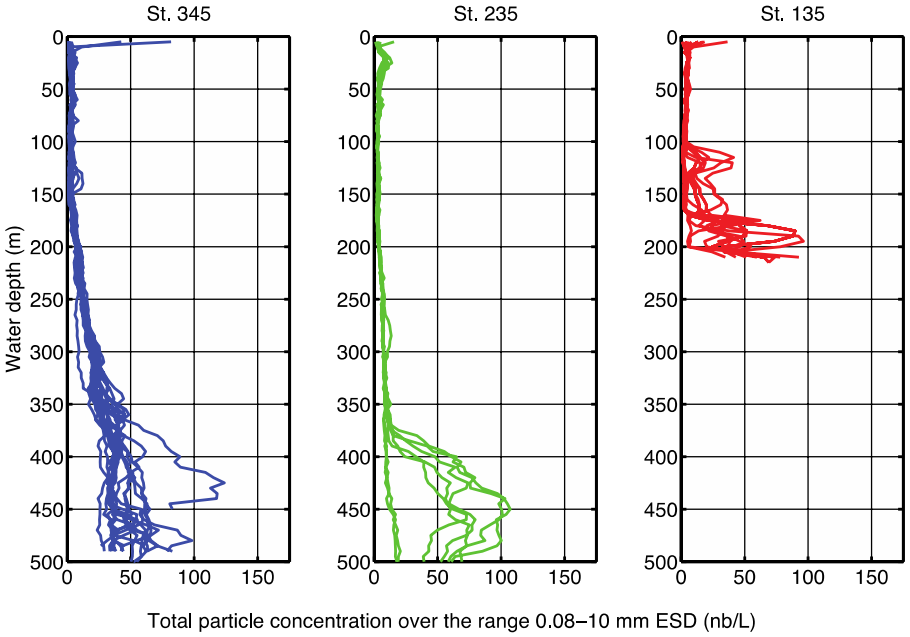

Figure 3. Vertical profiles of total particle concentration (in the size range 0.08–10 mm, in equivalent spherical diameter, ESD) measured at the drifting mooring sites and obtained with multiple deployments of the Underwater Vision Profiler 5.

BGD
12, 1247–1283, 2015

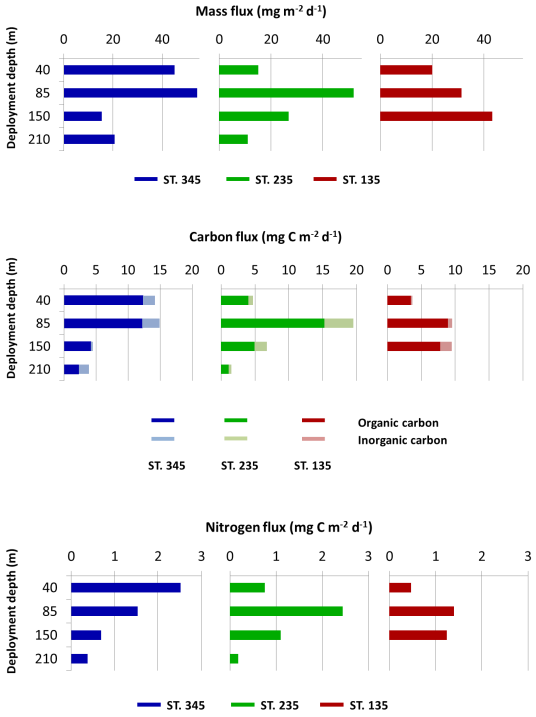

Figure 4. Downward flux of mass, particulate carbon (POC, PIC and TC, the sum of both) and particulate nitrogen obtained from drifting sediment trap moorings. Colours correspond to sites in Fig. 1.

BGD
12, 1247–1283, 2015

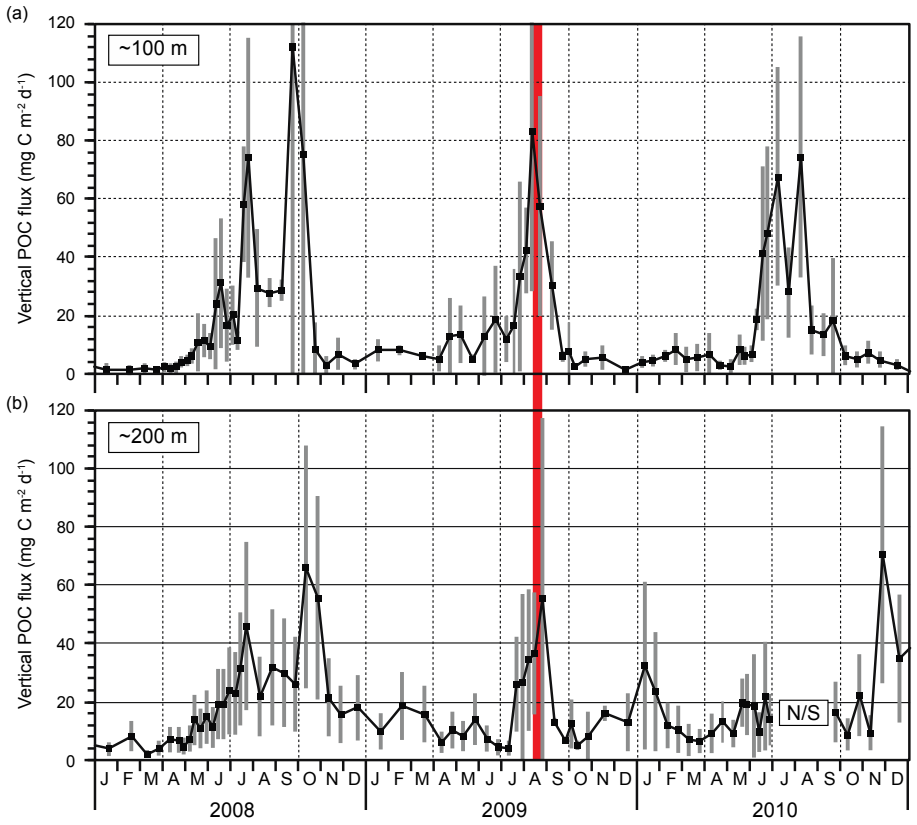

Figure 5. Times series of mean downward POC fluxes as measured at **(a)** ~ 100 m and **(b)** ~ 200 m with the ArcticNet sequential sediment traps (A1, G09, CA05, CA08 and CA16) moored in the vicinity of the drifting stations (see Fig. 1, Table 2). Vertical grey bars depict the standard deviation associated with each mean POC flux data point. The vertical red bar delimits the third week of August 2009 when short-term traps were deployed. N/S: no sampling.

BGD
12, 1247–1283, 2015

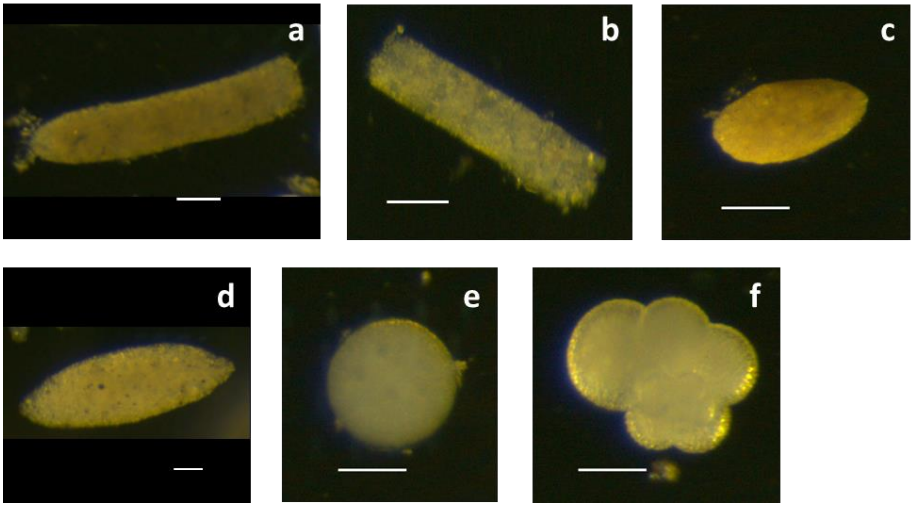

Figure 6. Large particles present in sediment traps: cylindrical faecal pellets (**a**: full, **b**: partly filled), elliptical pellets (**c**: full, **d**: partly filled), fish eggs **(e)** and foraminifera **(f)**. White bar is 100 µm.

BGD
12, 1247–1283, 2015

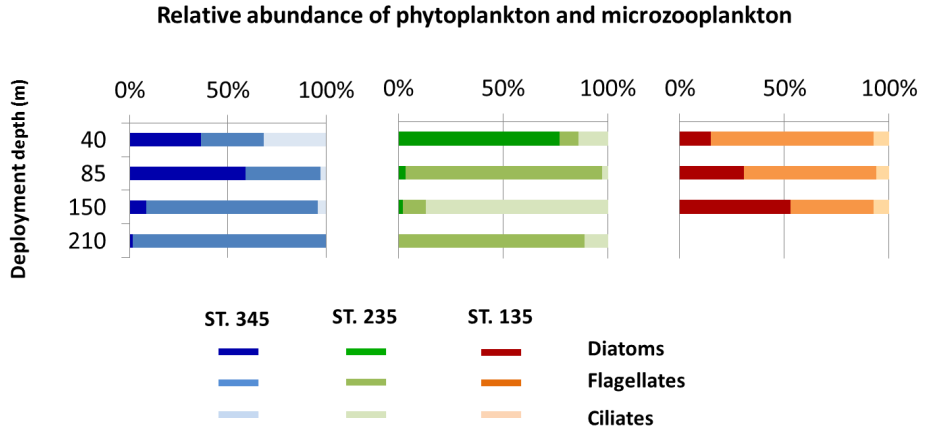

Figure 7. Relative contribution of phyto- and microzooplankton to the downward flux at different depths and stations. The identified taxa were grouped into diatoms, flagellates and ciliates.

BGD
12, 1247–1283, 2015